Journal of Superconductivity and Novel Magnetism (2019) 32:3915–3926
https://doi.org/10.1007/s10948-019-5095-3

ORIGINAL PAPER

Electronic and Magnetic Structure and Elastic and Thermal Properties of Mn_2-Based Full Heusler Alloys

Inshad Jum'h[1] · S. Sâad essaoud[2,3] · H. Baaziz[2,4] · Z. Charifi[2,4] · Ahmad Telfah[5,6]

Received: 16 February 2019 / Accepted: 30 March 2019 / Published online: 19 June 2019

Abstract

Magnetism, electronic structure, elastic and thermal properties of Mn_2YAl (with Y = Cr, V) have been investigated. The optimized lattice parameters, bulk modulus, and cohesive energy have been obtained. These alloys have the ferrimagnetic state as the most stable magnetic configuration, since the calculations showed a strong Mn-V antiferromagnetic coupling leading to the ferromagnetism of the Mn sublattices. A small and itinerant magnetic moment of Mn at the A site is found, which is antiparallel to the moment of Y at the B position in Mn_2YAl (with Y = Cr, V) compounds. The calculated total spin moments are integral values and increase from − 2 μ_B/f.u. for Mn_2VAl to − 1 μ_B/f.u. for Mn_2CrAl with increasing the number of valence electrons. Band structure and total and partial density of states could be calculated via applying the modified Becke Johnson approximation (mBJ). Based on these results, Mn_2YAl (with Y = Cr, V) are half-metallic ferrimagnets with the energy gap lies in the majority spin direction and a high-spin polarization (100%). The main difference between these two compounds is that the band gap is increased by 48% (0.210 eV for Mn_2CrAl and 0.401 eV Mn_2VAl). Elastic anisotropies, brittleness, and thermodynamic properties are determined for the Mn_2YAl (with Y = Cr, V). The slight difference in the spatial distributions of Young's moduli of Mn_2YAl (with Y = Cr, V) reflects the small differences for the elastic anisotropies of the alloys under consideration. The mechanical stability of Mn_2YAl (with Y = Cr, V) alloys are studied based on the elastic constants. The thermal properties are studied and investigated using the quasi-harmonic model, in addition, the temperature effect on heat capacities at constant pressure and volume, entropy, and thermal expansion are analyzed and discussed.

Keywords Heusler alloys · Half-metallic · Electronic structure · Ferrimagnetism · MBJ · Elastic constants · Mechanical stability · Anisotropic character

PACS 71.15.Mb · 71.15.-m · 65.40.Ba · 71.10.Hf · 65.40.gd

1 Introduction

Recently, half-metallic ferromagnets (HMFs) have been attracting much interest in spintronics applications [1, 2] such as spin injectors for magnetic random access memories [3]. Several new half-metallic ferrimagnets (HMFi) alloys have been designed for the development of low energy–consuming information. Among these materials, Heusler alloys have been considered among the most promising candidates, since being first discovered by the chemist Friedrich

✉ H. Baaziz
baaziz_hakim@yahoo.fr

✉ Z. Charifi
charifizoulikha@gmail.com

[1] School of Basic Science and Humanities, German-Jordanian University (GJU), Amman 11180, Jordan

[2] Department of Physics, Faculty of Science, University of M'sila, 28000 M'sila, Algeria

[3] Laboratoire de Physique des Particules et Physique Statistique, Ecole Normale Supérieure-Kouba, BP 92, Vieux-Kouba, 16050 Algiers, Algeria

[4] Laboratory of Physics and Chemistry of Materials, University of M'sila, M'sila, Algeria

[5] Leibniz-InstitutfürAnalytischeWissenschaften - ISAS - e.V, 44139 Dortmund, Germany

[6] Hamdi Mango Center for Scientific Research (HMCSR), The University of Jordan (UJ), Amman 11942, Jordan

Heusler when he studied and extracted the distinctive properties of the Cu_2MnAl compound [4]. After that, in 1983 de Groot et al. [5] revealed for the first time the half-metallicity in NiMnSb half-Heusler alloy, and since then several researchers have started to investigate other compounds such as Co_2MnZ [6].

Ternary Heusler alloys have the chemical formula X_2YZ, where X and Y are transition metals and Z is in the p-block; in some cases, Y is replaced by an alkaline earth metal. These materials are of great importance for their potential applications in electronic devices specifically, circuit boards and spintronic devices for the transfer, storage, and processing of electronic information [7, 8] and magnetoelectronics [9, 10]. Adding the spin degree of freedom to the conventional electronic devices based on semiconductors has potential advantages, like increased integration densities and decreased electric power consumption [9, 11].

In addition to their magnetic properties, Heusler alloys exhibit a high Curie temperature compared with the existing half-metallic materials [10]. The structural and magnetic properties of $Mn_2V_{1+x}Al_{1-x}$ have been studied in the whole range x [12], and it has been found experimentally that Mn_2VAl has a high Curie temperature (about 760 K [12]) and a small total magnetic moment (1.94 μ_B) and a nearly half-metallic alloy [9]. Itoh et al. [13] found that the stable phase is the ferrimagnetic state of Mn_2VAl compound, with $1.5 \pm 0.3\ \mu_B$ for the Mn magnetic moment and $-0.9\ \mu_B$ for the V moment [13]. This state is confirmed theoretically and reported by Weht and Pickett [14], who reported that for Mn_2CrAl the Curie temperature was equal to 549 K [15]. Wollmann et al. studied the Mn-based cubic compounds (among them, Mn_2VAl and Mn_2CrAl) and they showed that the structure type has no effect on the magnetic moments of manganese-rich Heusler compounds. The $L2_1$-type structure alloys are purely itinerant ferrimagnets with small magnetic moments on the Mn atoms that are coupled ferromagnetically [14]. Magnetism, half-metallicity, and Curie temperatures of Mn_2VZ (Z = Al, Ge) full Heusler alloys have been studied [16]. The calculations show that, although a large magnetic moment is carried by Mn atoms, Mn–Mn interactions in Mn_2VAl nearly cancel each other in the mean field experienced by the Mn atoms.

After the Co-based compounds, Mn_2YZ alloys are the second family that contains many HMFs. However, it is less studied compared with the first family. Mn_2VAl was defined as an HMFi and its magnetic properties are studied both experimentally and theoretically [13, 17]. Band structure investigations predict Mn_2VAl compound as a half-metallic ferrimagnet, i.e., with a limited gap in the density of states (DOS) for the spin up, whereas for the spin down the material behaves like a conductor.

Finding new functional materials is always tricky and searching for very exact properties (like half-metallicity) among a large group of Heusler alloys is even more difficult and needs the knowledge of physical properties, such as hardness, elastic constants, stiffness, anisotropic character, and mechanical stability. Two interesting compounds (Mn_2VAl and Mn_2CrAl) are being the focus of this study where we have investigated the site preference and their magnetic and electronic structure. The elasticity and thermal properties of these alloys are poorly known compared with the electronic structure at low temperature. For that reason, their elasticity and thermal properties are studied and analyzed in detail. Additionally, we inspect the elastic anisotropy of the compound and the effect of the Y atom on the studied properties using ab initio calculations with the full-potential linearized-augmented plane wave (FP-LAPW) method [17, 18].

Section 2 contains the details of the calculation and the method used to realize the study. The results discussed in this paper are presented in Sect. 3.1, 3.2, and 3.3, respectively. The zero-temperature ground-state results of the structural and magnetic characters of both Mn_2VAl and Mn_2CrAl are displayed in Sect. 3.1, and the electronic structure in terms of charge density, density of states, and band structures is in Sect. 3.2. Both elastic and thermal properties, such as specific heat at constant pressure and volumeC_p, C_v, entropy S, and thermal expansion α which are obtained from the non-equilibrium Gibbs energy are discussed in Sect. 3.3, and finally Sect. 4 summarizes our findings.

2 Crystal Structure and Computational Details

Both Mn_2CrAl and Mn_2VAl are ferrimagnetic materials, and they can crystallize in two-type structures according to the Mn atomic positions; The first type is $L2_1$-type structure (Cu_2MnAl structure, space group Fm-3m (225)) where the experimental lattice constants are equal to 5.71 Å for Mn_2CrAl [19] and 5.92 Å for Mn_2VAl [20]. The Wyckoff coordinates of X_2YZ full Heusler alloy are given as follows: the (0.25, 0.25, 0.25) and (0.75, 0.75, 0.75) positions for Mn, (0, 0, 0) for Al atoms, and (0.5, 0.5, 0.5) for Y (Cr or V) atoms. The other type is X_α (Hg_2CuTi-type) with space group F-43m (216), and Wyckoff coordinates corresponding to each atoms composed the X_2YZ full Heusler alloy are given as follows: (0.5, 0.5, 0.5) and (0.25, 0.25, 0.25) positions for Mn, (0.75, 0.75, 0.75) for Y (Cr or V) atoms, and (0, 0, 0) for the Al atoms [15]. Generally, the atoms with more valence electrons tend to occupy the A and C sites and form a Cu_2MnAl structure type (our case); while atoms with less electrons prefer the B sites and form a Hg_2CuTi-type structure. It is reported [13, 17] and confirmed in this work that in Mn_2YZ, Mn atoms enter the A and C sites contrary to the majority of the Heusler alloys, in which the Mn atom usually occupy the B site. V and Cr atoms located on the B sites and the D site corresponds to the Al atom.

Additionally, the properties of Mn_2YAl (with Y = Cr, V) were investigated by employing the full-potential linearized-augmented plane wave (FP-LAPW) method incorporated into Wien2k code [21]. The approximate exchange-correlation potentials are evaluated within the generalized gradient approximation parameterized by Perdew-Burke-Ernzerhof (GGA-PBE) [22] and the local density approximation (LSDA) [23]. We divided the unit cell into two regions; inside the no overlapping atoms sphere, in this case, the charge density and the potential are expressed via spherical harmonic expansion, so, we had chosen 2.0–2.2 a.u. as R_{mt} radius of Mn, Al, and Cr (V) atoms. In the interstitial region (outside the atomic spheres), we used the plane wave basis cutoff of $R_{mt}{}^{*}K_{max}$ equal to 9.0 for both compounds. Seventy-two special *k*-points for both alloys in the irreducible wedge of the Brillouin zone have been used to minimize the total energy.

The electronic configurations (for valence electrons) are for Mn: $3P^6 3d^5 4S^2$, for Al: $3s^2 3p^1$, and for Cr: $4s^1 4p^0 3d^5$ and V: $4s^2 4p^0 3d^3$. The separation energy between the valence and core states was set to − 81.63 eV. The charge convergence was set to $10^{-3}$and simultaneously energy convergence criterion was set to 10^{-5}. In addition, the electronic properties are calculated within the modified Becke Johnson approximation (mBJ) [24] which serves for optimization of the corresponding potential for electronic band structure calculations. The quasi-harmonic GIBBS2 code [25, 26] has been employed in order to calculate the thermal properties and for more details see ref. (Berarma et al. [27]).

3 Results and Discussions

3.1 Structure and Magnetic Ground State

Total energy calculations of Mn_2YAl (with Y = Cr, V) Heusler alloys have been carried out for two magnetic configurations; the first one is nonmagnetic (paramagnetic), and the second one is the magnetic (ferrimagnetic) phase. The equilibrium structural parameters for both Mn_2CrAl and Mn_2VAl alloys in ferrimagnetic (FMi) and paramagnetic phases have been calculated through minimizing the total energy of a primitive cell as a function of its volume. This work was performed by fitting the results with the Murnaghan equation of state [28]. Our results are summarized and compared with the available theoretical and experimental results in Table 1. This approximation is considered inaccurate for both compounds, since the calculated lattice parameters using LSDA approximation are far from the experimental results [19, 20] and other theoretical data [10, 14, 16]. However, the lattice constants calculated using GGA approximation are in good agreement with the reported results [15]. Remarkably, the Mn_2CrAl lattice constant is slightly smaller than that of Mn_2VAl due to the smaller atomic radius of Cr than that of V. For both compounds, the GGA approximation is used in the following. Thus, the energy curves as a function of volumes are shown in Fig. 1**,** for the two compounds in ferrimagnetic and paramagnetic phases in both types of structure ($L2_1$ and X_α). The energy of the ferrimagnetic $L2_1$-type structure becomes lower than that of the X_α-type structure at the optimized lattice parameter, which indicates that the (FMi) phase is more stable, with a difference in energy equal to 0.38 eV and 0.96 eV for Mn_2CrAl and Mn_2VAl, respectively (all the following results are calculated for the $L2_1$-type structure). It is difficult to form X_α-type structure in Mn_2YAl (Y = V, Cr) compounds since the total energy difference between the $L2_1$-type structure and X_α-type structure is too large, so the X_α phase is considered a metastable phase.

The bulk modulus *B* is a measure of the substance's resistance to uniform compression and is presented in Table 1. Indeed the values of B obtained (between 188 and 204 GPa) confirm the high hardness of the considered compounds. The cohesive energy is the amount of energy evolved when a crystalline solid is formed from infinitely

Table 1 Calculated equilibrium lattice constants, bulk modulus, and cohesive energy for Mn_2CrAl and Mn_2VAl compounds obtained by using SLDA and GGA

Compounds		GGA			SLDA			E_{coh}(eV/Mn_2YAl) (FMi ($L2_1$) GGA
		FMi ($L2_1$)	FMi (X_α)	PM	FMi ($L2_1$)	FMi (X_α)	PM	
Mn_2VAl	a (Å)	5.81	5.92	5.77	5.68	5.68	5.65	17.72
	B (GPa)	188.03	115.54	213.51	247.10	211.10	242.26	
	a_{exp} (Å)				5.92 [20]			
	a(Å)*			5.932 [16]	5.87 [14]			
	$\frac{\Delta a}{a}\Big\vert_{exp}$	0.019	0.000	0.025	0.041	0.041	0.046	
Mn_2CrAl	a (Å)	5.73	5.85	5.70	5.60	5.63	5.59	15.8
	B (GPa)	204.66	126.11	226.24	242.52	189.35	261.12	
	a_{exp} (Å)				5.71 [19]			
	a (Å)*				5.85 [29]	5.82 [14]		
	$\frac{\Delta a}{a}\Big\vert_{exp}$	− 0.004	− 0.025	0.002	0.02	0.01	0.021	

* Other work

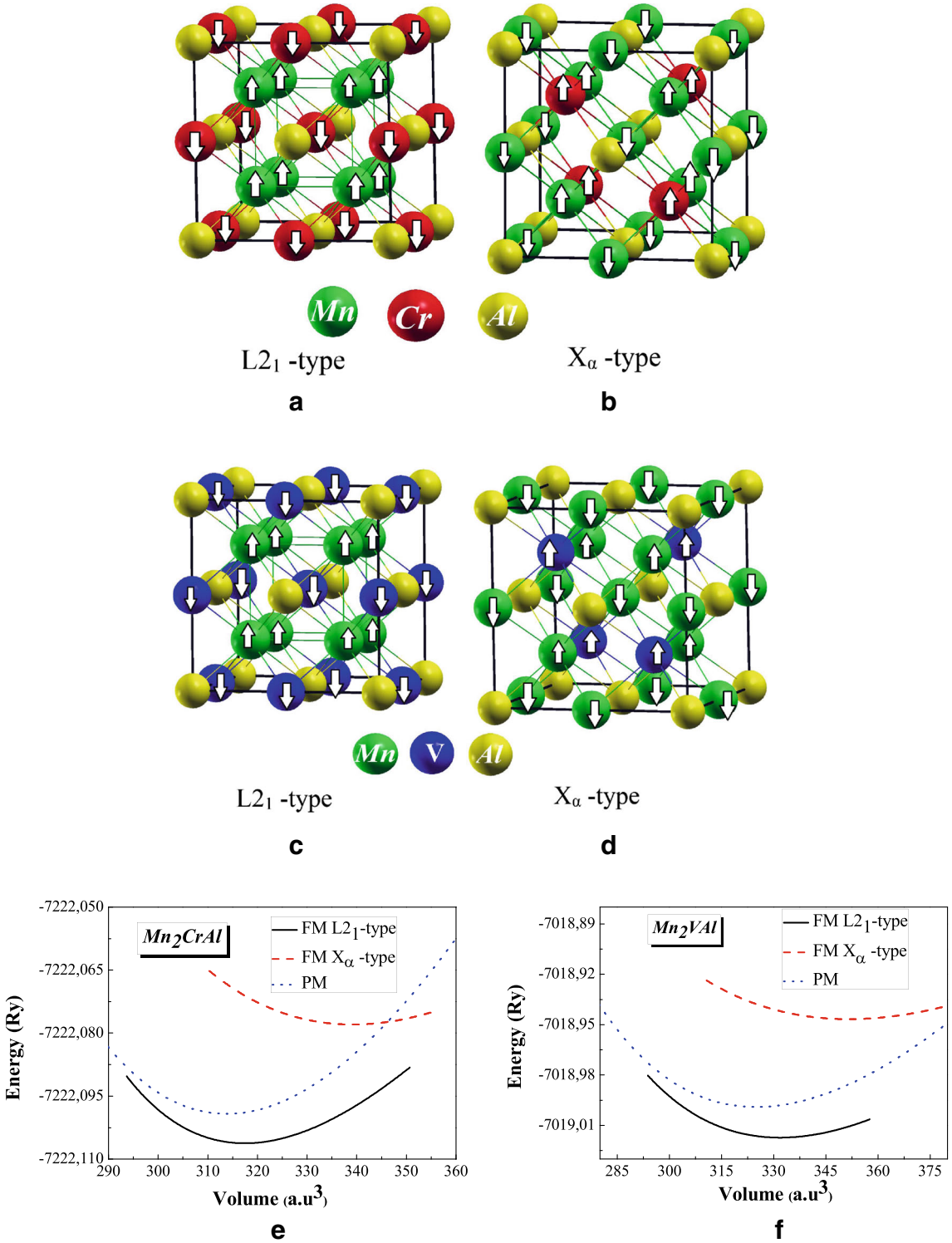

Fig. 1 Crystal structure of Mn_2YAl (Y = Cr, V) compounds in $L2_1$- and X_α-type structures (**a**–**d**). The volume dependence of total energy for Mn_2CrAl and Mn_2VAl compounds using GGA approximation (**e**–**f**)

separated atoms and it describes the measurement of the strength of the forces that bind atoms together in the solid state. The physical stability of Mn_2YAl (with Y = Cr, V) Heusler alloys can also be studied via the cohesive energy calculated using Eq. (1) and from the results obtained we can say that the atoms Mn_2VAl are more coherent than Mn_2CrAl compound.

$$E_{coh} = \left(2\,E_{atom}^{Mn} + E_{atom}^{Y} + E_{atom}^{Al}\right) - E_{tot}^{Mn_2YAl} \quad (1)$$

Where $E_{tot}^{Mn_2YAl}$ is the total energy of Mn_2YAl at the equilibrium and $E_{atom}^{Mn}, E_{atom}^{Y}, and\ E_{atom}^{Al}$ are defined as the atomic energies of Mn and Y atoms.

Table 2 shows for both compounds the total and the partial magnetic moments and spin polarization ratio at the equilibrium lattice constant in both type structures, $L2_1$ and X_α. Obviously, obtained results are in good agreement with results in [19, 29, 30, 32]. In addition, the total magnetic moment has integer values of − 2 μ_B and − 1 μ_B for Mn_2VAl and Mn_2CrAl, respectively. Our results agree with the Slater Pauling law [33, 34] which states that $M_{total} = N_v$-24 (where N_v is the number of valence electrons for compounds and it was equal to 22 and 23 for Mn_2VAl and Mn_2CrAl, respectively). Moreover, it has been found that the magnetization of Mn_2 systems does not exceed 2 μ_B/f.u., while in some rare cases it can reach 4 μ_B [15]. Interestingly, Heusler alloys having X_2YZ chemical formula where Y is an Mn atom (X_2MnZ), the compound have high-spin magnetic moment around 4 μ_B [14], whereas in the X site in Mn_2YAl, it has been obtained in our calculations that it has a low-spin magnetic moment (1–2 μ_B), in accordance with previous works.

All Mn moments in $L2_1$-type structure are parallel; however, the V moments are aligned oppositely, so the formation of the ferrimagnetic phase is determined by the strong antiferromagnetic coupling between the nearest Mn and V moments. The interactions between V atoms are very small and can be neglected [16]. The total magnetic moment is found to increase (from 1.038 to 1.999 μ_B) with replacing Cr by V and with decreasing the number of valence electrons in the unit cell (from 23 to 22), respectively. We have to mention that the alloys are predicted as half-metal ferrimagnets with an integral magnetic moment of about 1 and 2 μ_B (taking into account the errors of the calculations) for Mn_2CrAl and Mn_2VAl, respectively. The spin magnetic moments of Mn is aligned antiparallel to that of V (Cr) atom in Mn_2YAl (with Y = Cr, V) Heusler alloys. It is also shown that Mn in the position (A) atom has the largest local magnetic moment in the studied compounds (see Table 2). Spin polarization (P) gives as a good overview about the electronic behavior and it is defined by $P = \frac{(N_\uparrow(E_F) - N_\downarrow(E_F))}{(N_\uparrow(E_F) + N_\downarrow(E_F))}$, where $N_\uparrow$ and $N_\downarrow$stands for the density of states (DOS) in the (up or down) spin state at the Fermi energy (E_F).

The calculated spin polarization for both compounds is equal to 100 which confirms the reported results [19]. The $L2_1$-type Heusler alloys are purely itinerant ferrimagnets with small magnetic moments on the Mn atoms that are coupled ferromagnetically. The contributions of Y atoms to the total

Table 2 Calculated partial and total magnetic moments and spin polarization ratio at the equilibrium lattice constant Mn_2CrAl and Mn_2VAl compounds using GGA

Compounds	Our work							Other works				
	Mn_A (μ_B)	Mn_B (μ_B)	Al (μ_B)	Y (μ_B)	Intertitiel zone (μ_B)	Tot (μ_B)	P (%)	Mn (μ_B)	Al (μ_B)	Z (μ_B)	Tot (μ_B)	P (%)
Mn_2VAl ($L2_1$-type)	− 1.404	− 1.404	0.0147	0.741	− 0.054	− 1.999	100	− 1.84 [19]	0.18[19]	1.5[19]	−2.00[19]	100[19]
								− 1.41 [30]		0.77[30]	−2.00[30]	100[30]
								− 1.41 [31]		0.79[31]	−2:02[31]	
								− 1.52 [32]		0.95[32]		
Mn_2VAl ($X\alpha$-type)	− 2.008	2.211	0.006	1.375	0.372	1.957	100	− 3.02(A) [19], 3.18 (B) [19]	0.2[19]	−2.36[19]	−1.99[19]	100[19]
Mn_2CrAl ($L2_1$-type)	− 1.015	− 1.015	0.0023	0.946	− 0.030	− 1.038	100	− 1.03 [30]		1.00[30]	−1.04[30]	100[30]
Mn_2CrAl ($X\alpha$-type)	− 2.566	1.546	−0.005	1.801	0.223	1.00	100	− 1.70 [19]	0.08[19]	2.32[19]	−1.00[19]	100[19]
								2.81 (A) [29]	0.09[29]	−2.23[29]	−1.00[29]	
								− 1.68(B) [29]				

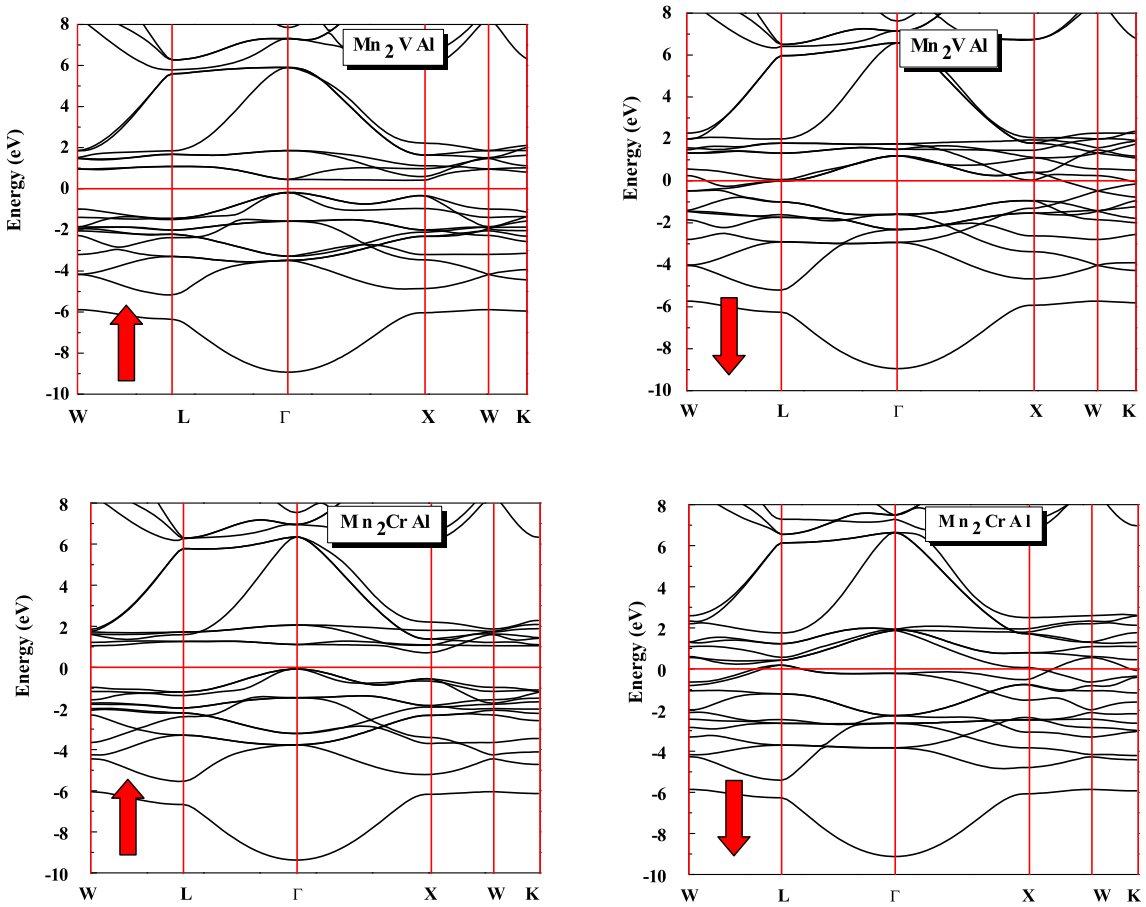

Fig. 2 Calculated band structures for the Mn_2YAl (Y = Cr, V) compounds by using MBJ approximation

moment are of minor importance and they are coupled antiparallel to the Mn moments.

3.2 Electronic Structure

Figure 2 illustrates the obtained band structure along high symmetry directions in the Brillouin zone treating the exchange-correlation term within mBJ approximation. The top of the valence band is at Γ and the bottom of the conduction band is located at the X point for the spin up. The density of state at the Fermi level is equal to zero in the spin-up case. Accordingly, Mn_2YAl (with Y = Cr,V) are half-metallic compounds with a band gap in the spin-up channel with Γ–X indirect band gap of about 0.210 eV for Mn_2CrAl and 0.401 eV for Mn_2VAl. The calculated gap using GGA approximation is found to be 0.25 eV for Mn_2VAl, and the Fermi level is at the top of the valence band in addition to a pseudo gap with a little number of states for Mn_2CrAl at Gamma point (0.164 states/eV). Within mBJ approximation, Mn_2YAl (with Y = Cr, V) shows a half-metallic behavior while Mn_2CrAl shows a metallic according to the performed GGA approximation. No significant difference is observed except that the gap in the majority bands at the Fermi level E_F has been increased by approximately 50% moving from Mn_2CrAl to Mn_2VAl using mBJ approximation.

The Fermi level shifts from the top to the middle of the gap for Mn_2VAl when we change the approximation from GGA to mBJ. This gap is mainly due the overlap of 3d states of Mn and Cr (V in Mn_2VAl). It is easily seen that their electronic structures are rather similar, and they all have an energy gap in DOS up. Noticeably, the gap width is quite sensitive to the lattice parameters and increases with the expanded lattice, which is in agreement with other theoretical results [35, 36]. We observe for Mn_2YAl (with Y = Cr, V) that the gap increases with the decrease of number d electrons when we compare the electronic configuration of Cr with V (see Fig. 3) around the Fermi level. Consequently, the lattice constant, the atom's electronegativity, and the number of valence electrons (3d atoms) are the main causes in the gap's modification.

The calculated total and partial density of states (DOS) using mBJ method for Mn_2YAl (with Y = Cr, V) in the two spin states (up and down) are plotted in Fig. 3. For both compounds, the minority spin band is strongly metallic, while the spin-up band is semiconductor-like around the Fermi level.

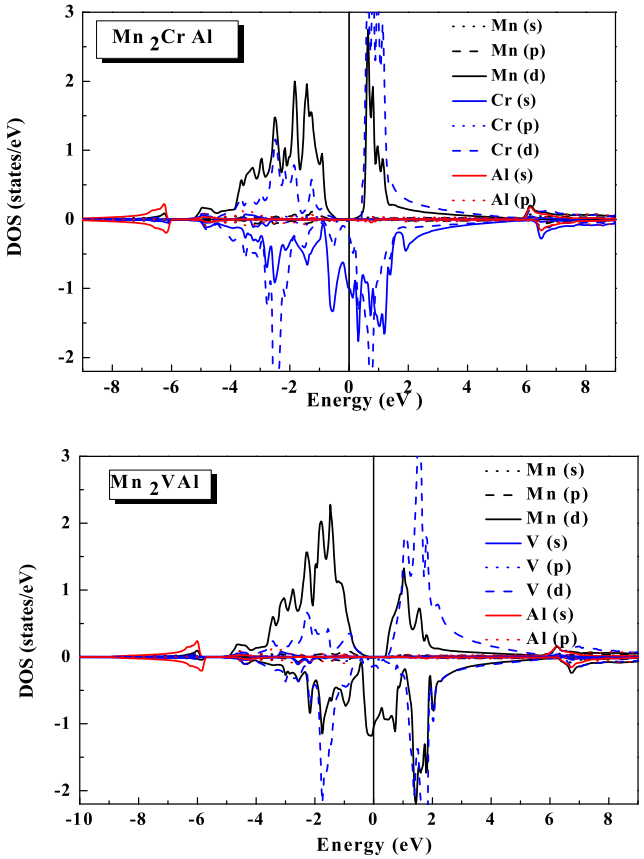

Fig. 3 Total and partial densities of states of the Mn_2YAl (Y = Cr, V) compounds

There is no DOS at the Fermi level for the spin-up state that indicates Mn_2YAl are half-metal ferrimagnets.

A high density of states at the Fermi level leads sometimes to a phase transition to lower symmetry. Sharp peaks in the DOS at the Fermi edge are indications of instabilities in the compound; accordingly, the Mn_2CrAl is more stable than Mn_2VAl. Correspondingly, the half-metallic character of these and other Heusler alloys with 22 (Mn_2VAl compound) conduction electrons is very easily destroyed by a slight deviation from stoichiometry or a small amount of atomic disorder. The bandgap locates in the spin up instead of the spin down in Mn_2CrAl and Mn_2VAl because they have valence electrons fewer than 24. The Fermi energy lies in the middle of the energy gap in Mn_2VAl and in the top of the valence band in Mn_2CrAl, accordingly the antisite disorder between the A, C, and the B sites or thermal excitation, lattice distortion can close the energy gap and destroy the half-metallicity in Mn_2CrAl. Fermi energy shifts from the maximum of the valence band to the inside of the bandgap with decreasing the number of valence electrons.

For Mn_2CrAl, from − 9.5 eV to − 6.2 eV, the contribution of 3s orbitals of Al atom for both directions of the spin is dominated and p states of the Al atoms are at − 5.5 eV. In Mn_2CrAl particularly, the Cr 3d–Mn 3d interactions exhibit a strong overlap (from − 5 to 4 eV). Due to the more complex d–d overlaps in these alloys, one has first to consider the interaction between the X elements. Although the symmetry of the $L2_1$ lattice is the tetrahedral one, the X elements themselves, if we neglect the Y and Z atoms, form a simple cubic lattice and sit at sites of octahedral symmetry [31]. The d-orbitals of the neighboring X atoms hybridize creating five bonding d-states, which after hybridizing with the d-orbitals of the Y atoms creates five occupied and five unoccupied d-hybrids and five non-bonding d-hybrids of octahedral symmetry (the triple-degenerated t_{1u} and double-degenerated e_u states). These non-bonding hybrids cannot couple with the orbitals of the neighboring atoms, since they do not obey the tetrahedral symmetry, and only the t_{1u} are occupied leading to 12 occupied spin-up states.

We mention that Mn_2VAl alloy has the same analysis as Mn_2CrAl and our obtained results are similar to other works [14, 19, 30]. For both compounds in spin up, there are gaps of energy and the total density of states at Fermi level is equal to zero whereas in the other spin direction there is a high DOS peak that confirms that these Heusler alloys have half-metallic character. In the total DOS of Mn_2VAl, there is a high unoccupied antibonding peak at about 1.6 eV in the minority spin states, but in Fig. 3a, the occupied bonding peak is high in the majority total DOS for Mn_2CrAl. The high minority antibonding peak in Fig. 3b is from the contributions of both Mn and V states while the high spin-up bonding peak in Fig. 3a is composed only of the bonding states of Mn (A).

The study of contour plots in planes provides useful information about the chemical bonding (Fig. 4 for spin up and spin down). The charge distribution around the constitutive atoms in (110) plan of a crystal is plotted in Fig. 4. The bonding charge density shows a depletion of the electronic density at the lattice sites together with an increase in the electronic density in the interstitial region. The bonding type of Mn-Cr and Mn-V is mostly covalent bonding in both compounds Mn_2CrAl and Mn_2VAl. As opposed to ionic bonding in which a complete transfer of electrons occurs, covalent bonding occurs when two (or more) elements share their electrons. This observation can be confirmed using the Pauling electronegativity of atoms composed of the full Heusler alloys Mn_2YAl which are equal to 1.55, 1.61, 1.66, and 1.63 for Mn, Al, Cr, and V atoms, respectively. In this study, and for both spins up and down, the two Heusler alloys exhibit a covalent bond. Based on the DOS graphs this covalent bonding is formed by the overlap of (3d) states of Mn and (3d) states of Cr in Mn_2CrAl and by the overlap of (3d) states of Mn and (3d) states of V in Mn_2VAl, and the electronic density increases in the interstitial region (Fig. 4).

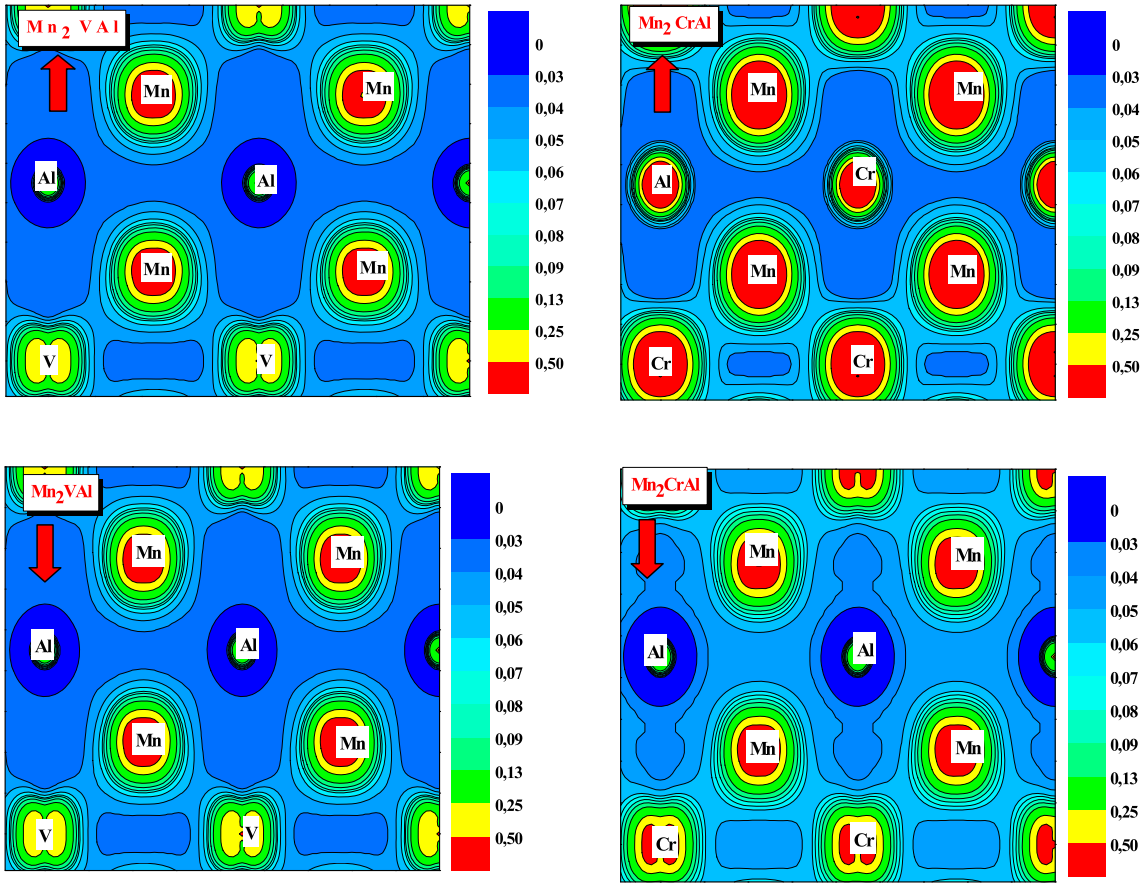

Fig. 4 Contour plot of valence charge density in (110) plane for Mn_2YAl (Y = Cr, V) compounds

3.3 Elastic and Thermal Properties

Elastic constants, which can be obtained from the second derivatives of the total energy, play an important role in the study of the crystal structure stability and its behavior under external forces therefore, accurate calculations of total energy are extremely important. In this study, elastic constants have been acquired from the total energy variation versus small strains, a numerical first principles calculation (calculate the total energy as a function of volume-conserving strains that break the cubic symmetry).The calculated elastic constants of Mn_2YAl (with Y = Cr, V) with $L2_1$-type structure are given in Table 3. Unfortunately, there are no experimental or previous theoretical results to compare with. Obviously, the bulk moduli calculated from elastic constants are in good agreement with those provided by the EOS equations (Table 1).

The cubic crystal has only three independent elastic constants, C_{11}, C_{12}, and C_{44}. Based on the obtained results (see Table 3), both Mn_2CrAl and Mn_2VAl compound verified the mechanic stability ($(C_{11}+2\ C_{12})>0$, C_{11}, C_{12}, and $C44>0$, $(C_{11}-C_{12})>0$, and $C_{12}<B_s<C_{11}$ [37]. From Table 3, it is found that C_{12} is smaller than C_{44}, indicating formation of covalent bonds, where the angular dependence of the interatomic forces becomes essential. The elastic moduli are found to be rather similar in both compounds. Moreover, detailed analysis of elastic parameters sheds light on phase transition and stability in Heusler alloys. For that other properties such as: C_s, Young modulus E, the anisotropy factor A and bulk modulus B, Poisson's ratio (v), and the isotropic Voigt's shear modulus G_V (deformation resistance) are also obtained (see Table 3). The mathematical relationship between the elastic constants and each of B, G, A, and E are given as follows [38]. For cubic crystals, the equations are expressed as following:

$$E = \frac{9\ \mathrm{B}\ \mathrm{G_v}}{3\ \mathrm{B} + \mathrm{G_v}} \tag{2}$$

$$A = \frac{2C_{44}}{C_{11}-C_{12}} \tag{3}$$

$$B = \frac{1}{3}(C_{11} + 2C_{12}) \tag{4}$$

$$C_s = \frac{1}{2}(C_{11}-C_{12}) \tag{5}$$

$$G_V = \frac{C_{11}-C_{12}+3C_{44}}{5} \tag{6}$$

$$v = \frac{3\ \mathrm{B}-\mathrm{E}}{6\ \mathrm{B}} \tag{7}$$

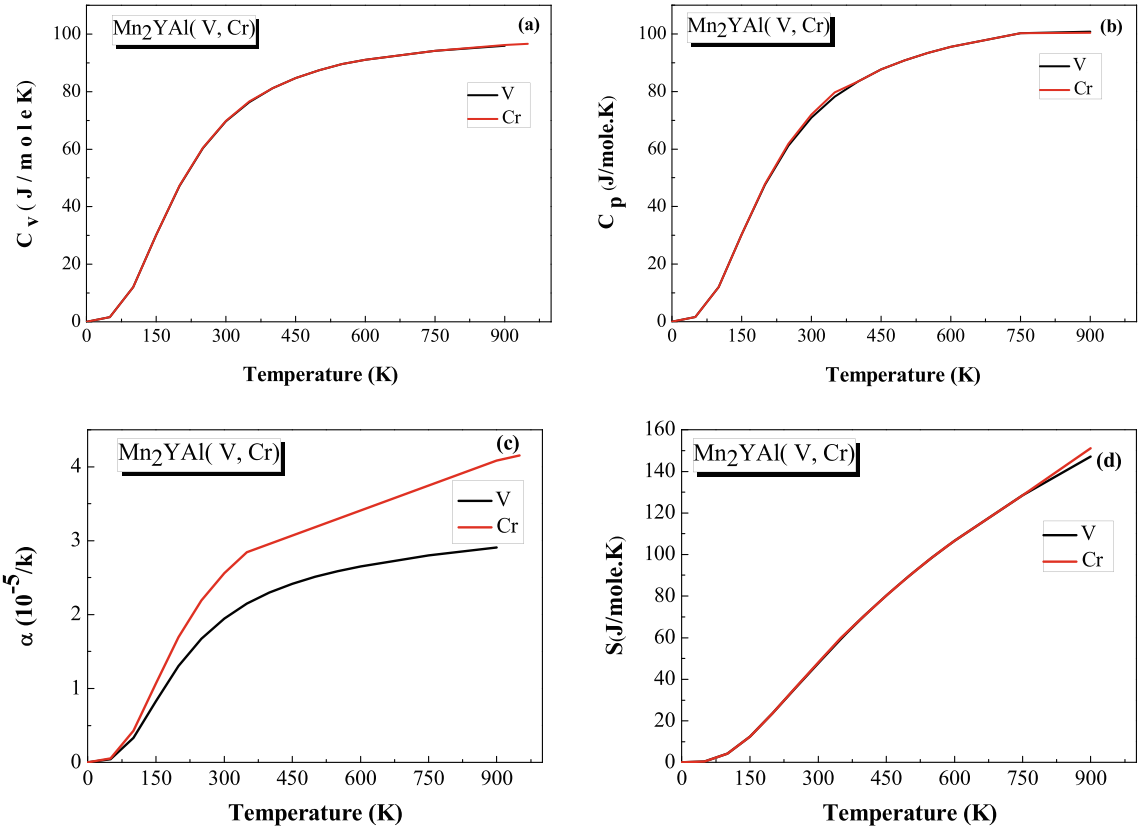

Fig. 5 Variation of heat capacities (C_V and C_P), entropy (S), and α parameters Mn_2YAl (Y = Cr, V) compounds as function of temperature

The factor A should equal to unity for isotropic crystals while any other values greater or smaller than unity is a measure of elastic anisotropy degree possessed by the crystal. Once the anisotropy factor A is greater than 1 then one can deduce that these crystals are harder in < 1, 1, 1 > direction. Pugh's ratio indicates the type of bonding, namely covalent or metallic bonding and for our compounds, Pugh's ratio (B/G) is less than 1.75 for both compounds, these small values indicating low malleability meaning the brittleness of the compounds. We also conclude that Mn_2CrAl is less brittle than Mn_2VAl (see Table 3). Also, we can see that the elastic constants calculated decrease when Cr is replaced by the V atom.

Poisson's ratio ν for covalent bonding is about 0.1 and increases for ionic crystals up to 0.25. So according to our results, the compounds are covalent ones. Anisotropy displays the tendency of a compound toward phase transitions. Indeed, an illustrative way to show the anisotropy is to visualize the Young's modulus (E). Three-dimensional surfaces, representing the dependence of the Young modulus on crystallographic directions are conducted in order to complete the investigation of the mechanical properties, which is a powerful approach to display the elastic anisotropy of a compound. The 3D closed surfaces that show the dependence of Young's modulus (E) on the crystallographic directions of a cubic crystal is defined as follows [39]:

$$\frac{1}{E} = S_{11} - 2\left(S_{11} - S_{12} - \frac{1}{2}S_{44}\right)\left(l_1^2 l_2^2 + l_2^2 l_3^2 + l_3^2 l_1^2\right) \quad (8)$$

Where: $S_{ij}=C_{ij}^{-1}$, $l_1 = \sin\theta\cos\varphi$, $l_2 = \sin\theta\sin\varphi$, and $l_3 = \cos\theta$ are the directional cosines with respect to the x, y, and z axes, respectively, where the two angles change between 0 and π for θ and 0 and 2π for φ. The obtained 3D closed surfaces of the Young's modulus of Mn_2CrAl and Mn_2VAl are presented in Fig. 6, respectively. It is shown that these surfaces are significantly far from spherical shape (see Fig. 6). Such significant

Table 3 Elastic constants, moduli of Young E, the anisotropy factor A, the adiabatic moduli of compressibility B, and the shear moduli of Mn_2YAl (Y = Cr, V)

	C_{11} (GPa)	C_{12} (GPa)	C_{44} (GPa)	C_s (GPa)	B (GPa)	G_V(GPa)	A (s.u)	E (GPa)	ν	B/G_v
Mn_2CrAl	298.63	141.53	243.89	78.54	193.89	155.08	3.10	408.45	0.15	1.25
Mn_2VAl	288.25	142.61	216.11	72.82	191.16	117.73	2.97	373.08	0.17	1.62

deviation from spherical shape (Fig. 6) designates that Mn_2YAl (with Y = Cr, V) alloys exhibit a large degree of anisotropy.

We also plotted the cross-sections of these surfaces in different planes (see Fig. 6a, b). From the 2D plane projections, one can see that the Young modulus at different planes has a large anisotropic character. Both Mn_2CrAl and Mn_2VAl compounds show a convex-concave shape. The noncircular shape of young modulus devoted at the spherical form by 75.34 GPa and 44.86 GPa for Mn_2CrAl and Mn_2VAl, respectively; however, Mn_2CrAl has a largest deviation compared with Mn_2VAl. The minimum values of Young modulus are along *x*, *y*, and *z* axis (see Fig. 6) while the maxima in the three xy, xz, and yz planes are along the diagonal direction. They take the values 282.96 GPa and 234.88 GPa for Mn_2CrAl and Mn_2VAl, respectively, thus deviation at the spherical form of young modulus decrease when Cr is replaced by V atom which implies that Mn_2CrAl compound is more susceptible to cracking compared with Mn_2VAl.

More information about the vibrational properties of solids can be attained based on studying heat capacity. The influence of temperature and pressure on the thermal properties of Mn_2YAl (with Y = Cr, V) has been studied using the quasi-harmonic Debye approach [26, 40] in this study. Our calculations are done in the temperature range of 0–1000 K. The temperature effects on: heat capacities (C_V and C_P), entropy (S), and α parameters are shown in Fig. 5. From Fig. 5, the heat capacity at volume constant checked the law of Petit-Dulong at high temperatures [41], while for both compounds C_v is proportional to T^3 at low temperature. At given pressure, C_v and C_p increased rapidly with increasing temperature and they decrease with increasing pressure. The thermal expansion coefficient alpha plotted versus temperature display alpha

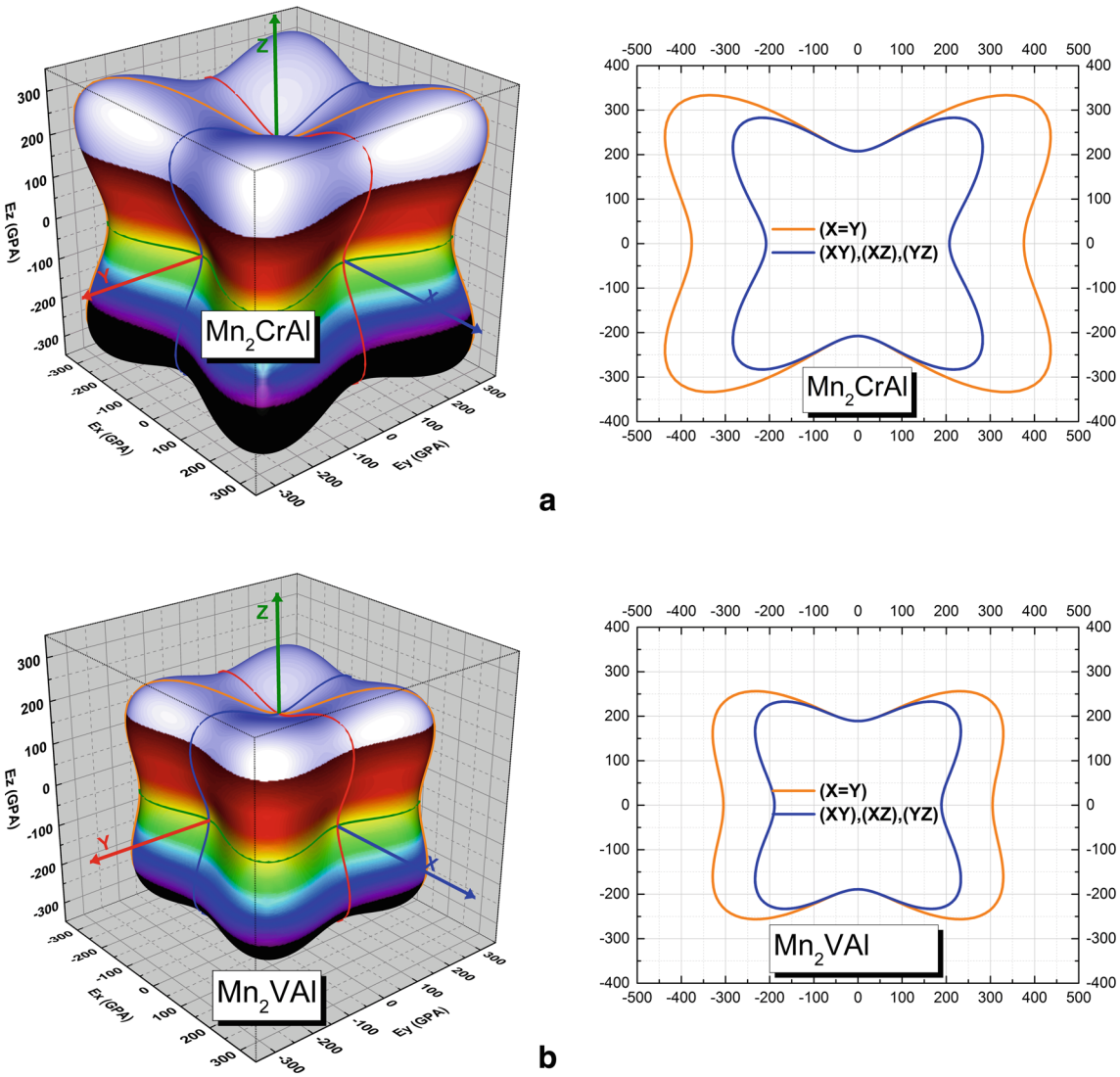

Fig. 6 3D representation of directional dependence of Young's modulus and cross-section in some reticular planes of 3D representation of (**a**) Mn_2CrAl and (**b**) Mn_2VAl

increasing with temperature increasing and at a given temperature, the thermal expansion decreases.

4 Conclusion

The electronic and magnetic structures of Mn_2YAl (with Y = Cr, V) Heusler alloys have been calculated and analyzed in order to explain their chemical bonding characteristics, magnetic configurations, and the elastic constants to study their stability, stiffness, and anisotropy. Mn_2YAl (with Y = Cr, V) is a new Heusler type, in which the Mn atom loses its preferential occupancy in the B sublattice, which is known generally for other Heusler type alloys X_2MnZ. Both Mn_2YAl (with Y = Cr, V) alloys show a ferrimagnetic state in which one Mn has the majority and the Y atom has the minority direction.

The present calculations indicate that the FMi in $L2_1$-type structure is more stable, with a difference in energy equal to 0.38 eV and 0.96 eV for the Mn_2CrAl and Mn_2VAl compounds, respectively. The structural results obtained, such as the lattice parameters and cohesive energy, are in good agreement with theoretical and experimental findings in the literature. The crystalline stability of Mn_2YAl has been investigated based on the calculations of their elastic properties. Mn_2YAl fulfills the physical stability condition and these compounds have a half-metallic electronic behavior with covalent chemical bonding. For the studied Heusler alloys, the elastic properties suggested the formation of covalent bonding with small malleability and brittleness. A significant deviation from the spherical shape indicates that Mn_2YAl (with Y = Cr, V) alloys exhibit a large degree of anisotropy. However, a slight difference is found for the elastic anisotropies of the compounds. These are reflected in the small spatial distributions of Young's moduli when comparing the compounds.

References

1. Julliere, M.: Tunneling between ferromagnetic films. Phys. Lett. A. **54**(3), 225–226 (1975)
2. Dieny, B., Speriosu, V.S., Parkin, S.S.P., Gurney, B.A., Wilhoit, D.R., Mauri, D.: Giant magnetoresistive in soft ferromagnetic multilayers. Phys. Rev. B. **43**(1), 1297–1300 (1991)
3. Ohno, H.: Making nonmagnetic semiconductors ferromagnetic. Science. **281**(5379), 951 (1998)
4. Heusler F.:Über magnetische Manganlegierungen. sl: Verhandlungen der Deutschen Physikalischen Gesellschaft, 5, p. 219 (1903)
5. de Groot, R.A., Mueller, F.M., Engen, P.G.V., Buschow, K.H.J.: New class of materials: half-metallic ferromagnets. Phys. Rev. Lett. **50**(25), 2024–2027 (1983)
6. Ishida, S., Masaki, T., Fujii, S., Asano, S.: Theoretical search for half-metalliic films of Co2MnZ (Z = Si, Ge). Phys. B Condens. Matter. **245**(1), 1–8 (1998)
7. Žutić, I., Fabian, J., Das Sarma, S.: Spintronics: fundamentals and applications. Rev. Mod. Phys. **76**(2), 323–410 (2004)
8. Schmidt, G., Molenkamp, L.W.: Spin injection into semiconductors, physics and experiments. Semicond. Sci. Technol. **17**(4), 310 (2002)
9. Prinz, G.A.: Magnetoelectronics. Science. **282**(5394), 1660 (1998)
10. W.P.J.a.Z.K.R. A.: Alloys and Compounds of d-Elements with Main Group Elements. Part 2 (Landolt B¨ ornstein New Series, Group III, Vol. 19, Pt.c) ed (Berlin: Springer) pp. 75–184, (1988)
11. Wolf, S.A., Awschalom, D.D., Buhrman, R.A., Daughton, J.M., von Molnár, S., Roukes, M.L., Chtchelkanova, A.Y., Treger, D.M.: Spintronics: a spin-based electronics vision for the future. Science. **294**(5546), 1488 (2001)
12. Yoshida, Y., Kawakami, M., Nakamichi, T.: Magnetic properties of a ternary alloy $Mn_{0.5}V_{0.5\text{-}y}Al_y$. J. Phys. Soc. Jpn. **50**(7), 2203–2208 (1981)
13. Itoh, H., Nakamichi, T., Ocirc, Yamaguchi, Y., Kazama, N.: Neutron diffraction study of Heusler type alloy $Mn_{0.47}V_{0.28}Al_{0.25}$. Trans. Jpn. Inst. Metals. **24**(5), 265–271 (1983)
14. Weht, R., Pickett, W.E.: Half-metallic ferrimagnetism in Mn_2VAl. Phys. Rev. B. **60**(18), 13006–13010 (1999)
15. Wollmann, L., Chadov, S., Kübler, J., Felser, C.: Magnetism in cubic manganese-rich Heusler compounds. Phys. Rev. B. **90**(21), 214420 (2014)
16. Şaşioglu, E., Sandratskii, L.M., Bruno, P.: First-principles study of exchange interactions and curie temperatures of half-metallic ferrimagnetic full Heusler alloys Mn 2 V Z (Z = Al, Ge). J. Phys. Condens. Matter. **17**(6), 995 (2005)
17. Ishida, S., Asano, S., Ishida, J.: Bandstructures and hyperfine fields of Heusler alloys. J. Phys. Soc. Jpn. **53**(8), 2718–2725 (1984)
18. Khmelevskyi, S., Shick, A.B., Mohn, P.: Element-specific analysis of the magnetic anisotropy in Mn-based antiferromagnetic alloys from first principles. Phys. Rev. B. **83**, 224419 (2011)
19. Hongzhi, L., Zhiyong, Z., Li, M., Shifeng, X., Xiaoxi, Z., Chengbao, J., Huibin, X., Guangheng, W.: Effect of site preference of 3d atoms on the electronic structure and half-metallicity of Heusler alloy Mn_2YAl. J. Phys. D. Appl. Phys. **41**(5), 055010 (2008)
20. Jiang, C., Venkatesan, M., Coey, J.M.D.: Transport and magnetic properties of Mn2VAl: search for half-metallicity. Solid State Commun. **118**(10), 513–516 (2001)
21. Blaha, K.S.P., Madsen, G.K.H., Kvasnicka, D., Luitz, J., WIEN2K: An Augmented Plane Wave Local Orbitals Program for Calculating Crystal Properties. Karlheinz Schwarz, Techn. Universitat, Wien (2011)
22. Perdew, J.P., Burke, K., Ernzerhof, M.: Generalized gradient approximation made simple. Phys. Rev. Lett. **77**(18), 3865–3868 (1996)
23. Kohn, W., Sham, L.J.: Self-consistent equations including exchange and correlation effects. Phys. Rev. **140**(4A), A1133–A1138 (1965)
24. Becke, A.D., Johnson, E.R.: A simple effective potential for exchange. J. Chem. Phys. **124**(22), 221101 (2006)
25. Otero-de-la-Roza, A., Abbasi-Pérez, D., Luaña, V.: Gibbs2: a new version of the quasiharmonic model code. II. Models for solid-state thermodynamics, features and implementation. Comput. Phys. Commun. **182**(10), 2232–2248 (2011)
26. Otero-de-la-Roza, A., Luaña, V.: Gibbs2: a new version of the quasi-harmonic model code. I. Robust treatment of the static data. Comput. Phys. Commun. **182**(8), 1708–1720 (2011)
27. Berarma, K., Charifi, Z., Soyalp, F., Baaziz, H., Uğur, G.: U. Ş, Investigation of electronic structure and thermodynamic properties of quaternary Li-containing chalcogenide diamond-like semiconductors. Semicond. Sci. Technol. **31**(12), 125015 (2016)
28. Murnaghan, F.D.: The compressibility of media under extreme pressures. Proc. Natl. Acad. Sci. **30**(9), 244 (1944)

29. Skaftouros, S., Özdoğan, K., Şaşıoğlu, E., Galanakis, I.: Generalized Slater-Pauling rule for the inverse Heusler compounds. Phys. Rev. B. **87**(2), 024420 (2013)
30. Haraguchi, K., Fujii, S., Ishida, S., Asano, S.: Electronic structure of Cr–Mn–V–Z system based on Heusler Mn_2VZ (Z = Al, Ga). J. Phys. Soc. Jpn. **81**(7), 074710 (2012)
31. Galanakis, I., Dederichs, P. H.: Slater-Pauling Behavior and Origin of the Half-Metallicity of the Full-Heusler Alloys, pp. 1–9, (2002)
32. Sabine, W., Hem, C.K., Gerhard, H.F., Claudia, F.: Valence electron rules for prediction of half-metallic compensated-ferrimagnetic behaviour of Heusler compounds with complete spin polarization. J. Phys. Condens. Matter. **18**(27), 6171 (2006)
33. Pauling, L.: The nature of the interatomic forces in metals. Phys. Rev. **54**(11), 899–904 (1938)
34. Slater, J.C.: The ferromagnetism of nickel. II. Temperature effects. Phys. Rev. **49**(12), 931–937 (1936)
35. Luo, H., Zhu, Z., Liua, G., Xu, S., Wu, G., Liu, H., Qu, J., Li, Y.: Prediction of half-metallic properties for the Heusler alloys Mn2CrZ(Z = Al, Ga, Si, Ge, Sb): a first-principles study. J. Magn. Magn. Mater. **320**, 421–428 (2008)
36. Santao Qi, C.-H.Z., Chen, B., Shen, J.: First-principles study on the band structure, magnetic and elastic properties of half-metallic Mn_2CrAl. Mod. Phys. Lett. B. **29**, 1550139 (2015)
37. Born, K., Huang, M.: Dynamical Theory of Crystal Lattices. Clarendon, Oxford (1956)
38. Jamal, M., Jalali Asadabadi, S., Ahmad, I., Rahnamaye Aliabad, H.A.: Elastic constants of cubic crystals. Comput. Mater. Sci. **95**, 592–599 (2014)
39. Nye, J.F.: Properties of Crystals. Oxford Univ. Press, NewYork (1985)
40. Debye, P.: Einige Bemerkungen zur Magnetisierung bei tiefer Temperatur. Ann. Phys. **386**(25), 1154–1160 (1926)
41. Dulong, P.L., Petit A.T.: Recherches Sur Quelques Points Importans de La Theorie de La Chaleur Ann. Chim. Phys. 10–395 (1819).